京都大学防災研究所年報 第 50 号 B 平成 19 年 4 月
Annuals of Disas. Prev. Res. Inst., Kyoto Univ., No. 50 B, 2007

Ripple Formation and Grain Sorting with Multiple-sized Sand: a Report of the Preliminary Wave-flume Experimentation

Naofumi YAMAGUCHI* and Hideo SEKIGUCHI

*Graduate School of Science, Kyoto University

Synopsis

Three series of wave-flume experiments were performed for the purposes of assessing capability of a wave-flume and investigating an effect of multiple-sized sand on ripple formation. The first series of experiments were performed under fixed-bed condition, indicating that the measured performance of wave height-to-stroke ratio was only slightly smaller than theoretically expected. The other two series with multiple-sized sand beds facilitated the following: (1) the critical value of the mobility number for ripple formation with multi-sized sands may be larger than the critical value with uniform sands; and (2) as more asymmetrical oscillatory flow, the difference of grain size between onshore-slope and offshore-slope appeared more prominently.

Keywords: wave ripple, wave-flume experiments, multiple-sized sand, asymmetrical oscillatory flow, grain sorting

1. Introduction

Coastal sediments have an extensive range of grain sizes. Despite this universally accepted observation, most of the previous studies concerning coastal sediment transport and depositional processes have focused on uniform material for simplification. The performance of multiple-sized materials has often been explained in the terms of an apparently straightforward generalization of the results that were obtained for the simpler uniform cases. The importance of studying the relevant problem about the transport and deposition of multiple-sized materials has recently been well recognized such as selective sediment transport. Indeed, a careful investigation into the effect of selective sediment transport, which may enhance the process of grain-size sorting, may lead to a full understanding of bottom morphology in shallow-water environments. However, only a few studies (Foti, 1993; Foti and Blondeaux, 1995) have investigated the development of ripples and grain-sorting processes on ripple surfaces, although ripples develop well in shallow water. The ripple formation under various wave conditions, involving asymmetric oscillatory flow inherent in waves in the shallow-water region, remains to be explored further.

Thus, this experimental study using wave-flume will focus on grain sorting on ripples under various-wave conditions.

2. Laboratory experiment

2.1 Wave flume

The wave flume used is 34 m long, 0.4 m wide and 1.2 m deep (Fig. 1). It was initially designed by Fujio Masuda at the Division of Earth and Planetary Science, Kyoto University for examination of storm-generated bedforms such as hummocky bed (Southard et al., 1990). When it was recently transferred to the Disaster Prevention Research Institute, Kyoto University, decisions were made to introduce the following three adaptations: (1) extension of the flume length by 9 m,

Fig. 1 Photograph of the wave flume

(2) provision of a piston-type wave generator and (3) installation of a wave-dissipating slope whose dip can be changed. The period of oscillation and stroke (maximum position limit: ± 50 cm) of the piston-type wave generator with a 5 kw-AC servo motor are controlled through a digital function generator (NF Corporation DF1906). The upgraded wave generator allows flexible setting of wave conditions and longer-duration experiments if necessary. The wave-dissipating slope permits dips in the range of 1/18–1/5, along with the placement of wave-energy absorber on it. The wave absorber is commercially available and it called 'Hechimalon' (Shinko Nylon Corporation).

2.2 Methods and materials

The present experimental program consisted of 3 series of experiments, each of which comprised several runs. The first series composed of 83 runs was performed with fixed-bed conditions. The water depth ranged from 30 to 55 cm, the wave period from 0.80 to 10.00 s, and wave height from 5.6 to 28.4 cm. Each run had at least 30-min wave action to confirm whether the wave generator worked within its performance limitation.

The other two series composed of 47 runs were carried out on a sand bed (2.5 m long, 40 cm wide, and 8 cm thick; Fig. 2a). The water depth over the sand bed ranged from 30 to 50 cm. The wave period ranged from 1.25 to 5 s, and wave height from 3.8 to 20.6 cm. In all of the experiments, the dip of the wave-dissipating slope was set up as 1/18.

In the present experimental program, the authors used multiple-sized sand as the bed material. The multiple-sized sand was obtained by mixing two kinds of well sorted quartz sands which had different grain-size distributions (Fig. 3). The two sediments, the coarse sand (red-colored sand, mean diameter D = 0.40 mm; black-colored sand, D = 0.84 mm) and the fine materials (quartz sand, D = 0.18 mm), were mixed with same weight. More specifically, two types of mixed sand were prepared: one is the mixture of red-colored sand and quartz sand (Mixture I; D = 0.267 mm) for the second series; and another is the mixture of black-colored sand and quartz sand (Mixture II; D = 0.387 mm) for the third series. Grain-size analyses of these sands were performed with a settling tube (Naruse, 2005).

Two types of initial bed surface were prepared: a horizontal flat bed and a notched flat bed (Fig. 2b). A notch formed on a sand bed may promote formation of ripple marks (Sekiguchi and Sunamura, 2004, 2005). Ripple formation in the present study was recorded using a digital video camera during each run, and photographs taken at the start and the end of each run. The characteristics of ripple geometry (e.g. ripple spacing) were measured with the photographs of vertical forms taken through the side glass.

3. Results and discussion

3.1 Experimental parameters

In this study, water depth, h, and wave height, H, were measured for a given pair of wave period, T, and wave board stroke, S_0, that specified the motion of the wave generator. These parameters enabled the

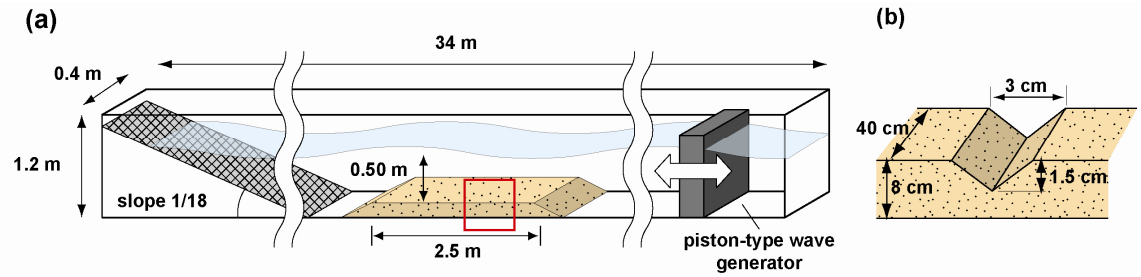

Fig. 2 (a) Wave flume used in this study. A sand bed was constructed in the horizontal portion of the flume. (b) schematic of a notch prepared on sand-bed surface

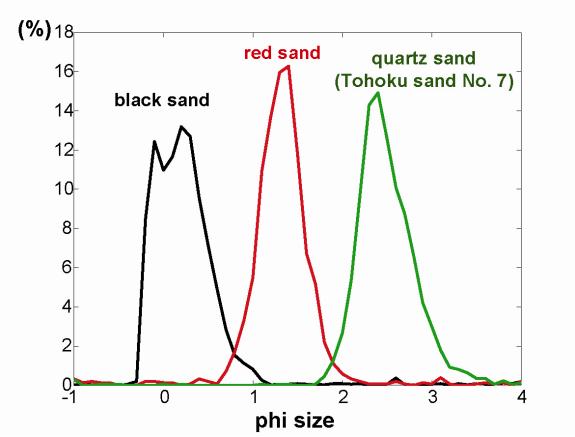

Fig. 3 Measured distributions of grain size in the three materials indicated

determination of some physical quantities for the hydraulic conditions.

According to linear wave theory (e.g. Dean and Dalrymple, 1992; Komar, 1998), the wavelength, L, the near-bottom maximum flow velocity, U_b, and the near-bottom orbital diameter, d_o, are calculated as:

$$L = \frac{gT^2}{2\pi}\tanh kh, \tag{1}$$

$$U_b = \frac{\pi H}{T\sinh kh} \tag{2}$$

and

$$d_o = \frac{H}{\sinh kh} \tag{3}$$

where g is the gravitational acceleration and k is the wavenumber which is given by $k = 2\pi/L$. The values of L, U_b and d_o were calculated replacing H by H_{max} in the first series of experiments, and H by $(H_{max} + H_{min})/2$ in the other two series.

The reflection coefficient, which indicates a rate of reflected wave to incident wave, was used here for representing the degree of wave-absorbing in each experimental condition. The reflection coefficient, R, is given by the following equation (Wiegel, 1964):

$$R = \frac{H_{max} - H_{min}}{H_{max} + H_{min}} \tag{4}$$

where H_{max} is a maximum wave height and H_{min} is a minimum wave height. When incident waves completely reflect from something like a vertical wall, for example, composite waves become pure standing waves and $R = 1$. While, the case of a purely incident wave corresponds to $R = 0$. The value of both H_{max} and H_{min} were measured at three runs in the first series of experiments and every run in the other series.

The theoretical wave-height was employed to compare with the observed wave-height for only first series of experiments. According to general first-order wavemaker solution for a piston-type wave generator (Dean and Dalrymple, 1992; Hughes, 1993), the wave height-to-stroke ratio is given by:

$$\frac{H}{S_0} = \frac{4\sinh^2 kh}{\sinh 2kh + 2kh}. \tag{5}$$

The theoretical wave-height was calculated through eq. (5).

For the second and third series of experiments, two dimensionless parameters were applied to analysis the data: namely, the mobility number, M, and the Ursell number, U. The mobility number, which is a simplified form of the Shields number, has been applied by many ripple studies (e.g. Dingler, 1975 Komar and Miller, 1975; Lofquist, 1978; Nielsen, 1979, 1981; Sekiguchi and Sunamura, 2004, 2005). The mobility number, M, is given by:

$$M = \frac{\rho U_b^{\,2}}{(\rho_s - \rho)gD} \tag{6}$$

where D is the sediment grain size, ρ_s and ρ are the densities of sediment grains and water, respectively.

The Ursell number, U, used here for representing degree of asymmetry of the orbital velocity near the bottom by shallow-water deformation, is given by (Ursell, 1953)

$$U = \frac{HL^2}{h^3} \tag{7}$$

The increase of U indicates more asymmetrical velocity: a larger onshore velocity of shorter duration and a smaller offshore velocity of longer duration in comparison to orbital velocity in a purely sinusoidal wave.

These data sets of the three series of experiments are summarized in Appendix of this paper.

3.2 Performance of the wave generator

In the first series consisting of 83 runs, 51 runs were normally performed during at least 30-min and 32 runs experienced the performance limits of the wave generator. In the normally-performed runs of this

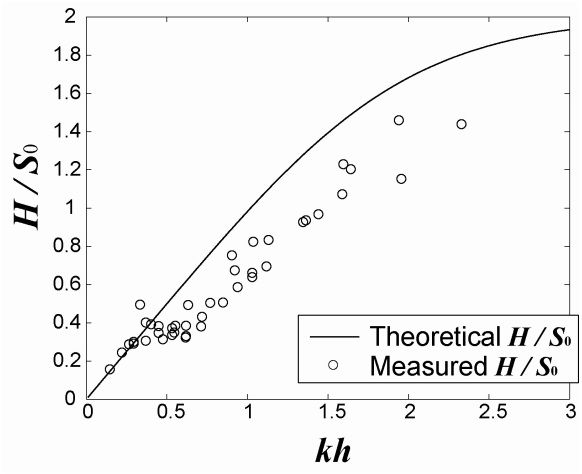

Fig. 4 Theoretical and measured wave height-to-stroke ratio, H/S_0, against wave number, kh

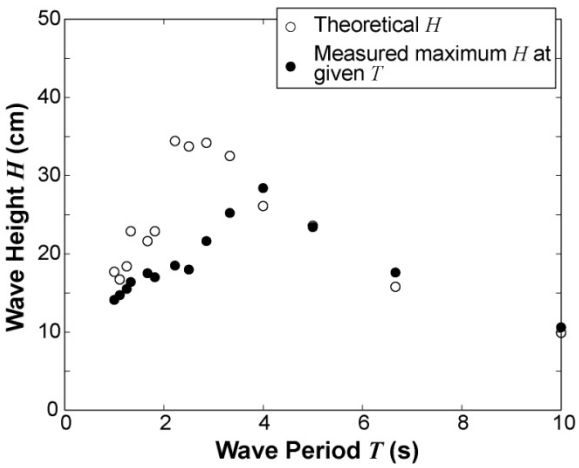

Fig. 5 Measured maximum H within the performance limitation of the wave-flume and theoretical H calculated through eq. (5) with measured So at given T. The water depth was 55 cm at each run

series, the wave length given by eq. (1) ranged from 1.0 to 23.6 m cm, the near-bottom maximum flow velocity by eq. (2) from 8.7 to 59.0 cm/s, and the near-bottom orbital diameter by eq. (3) from 1.4 to 39.8 cm.

Measured H / S_0 ratios are plotted against the dimensionless wave number specified (Fig. 4). In this figure the theoretical H / S_0 -kh curve is also plotted. Although the difference between measured and theoretical H / S_0 ratios became somewhat larger at large kh-values, the wave generator showed expected performance to some extent at relatively smaller kh-values, where experiments of ripple formation are often performed.

Measured maximum H which could be generated within the performance limitation of this wave-flume at h = 55 cm in relation to each given wave-period (1.0 ≤ T ≤ 10.0 s) is plotted (Fig 5), and was largest at T = 4.0 s (H = 28.4 cm). Measured maximum H was smaller than theoretical wave-height calculated through eq. (5) with measured S_0 for relatively shorter wave-period (T < 4.0 s) and about the same as it for relatively longer wave-period (T ≥ 4.0 s).

3.3 Ripple formation

In the second and third series of experiments consisting of 48 runs, ripples formed at 22 runs. In the other 26 runs, although sand particles moved, ripples did not developed within at least 30-min.

Mobility numbers M in relation to U in the notched-bed experiments were plotted for the purpose of comparing critical M-value for ripple formation with multiple-sized sand to one with uniform sand (Fig. 6). In the present experiments with multiple-sized sand, the curve in Fig. 6 is drawn through scattered data points showing "ripple formation" or "no ripple formation" to reasonably demarcate the two domains after Sekiguchi and Sunamura (2004), and may be expressed in the following equation:

$$M = 10.5 - 7.0e^{-0.04U} \tag{8}$$

where M-value was calculated with the mean grain diameter. The curve for ripple formation with uniform sand, given by Sekiguchi and Sunamura, 2004), was described as:

$$M = 5.0 - 2.5e^{-0.1U} . \tag{9}$$

The curve described as eq. (8) (i.e. for multiple-sized sand) was plotted above the curve described as eq. (9) (i.e. for uniform sand, Fig. 6). The difference of the two curves suggested that the critical value of the mobility number for multi-sized sands may be larger than the critical value of the uniform sands. This suggestion was consistent with Foti (1993), and Foti and Blondeaux (1995), which described that multiple-sized sand tends to prevent ripple development started from initially flat bed.

As U-value increasing (i.e. more asymmetrical), the difference of grain size between onshore-slope and offshore-slope appeared more prominently. The coarser sediments deposited on the onshore-side slopes than the offshore-side slopes (Fig. 7). The difference

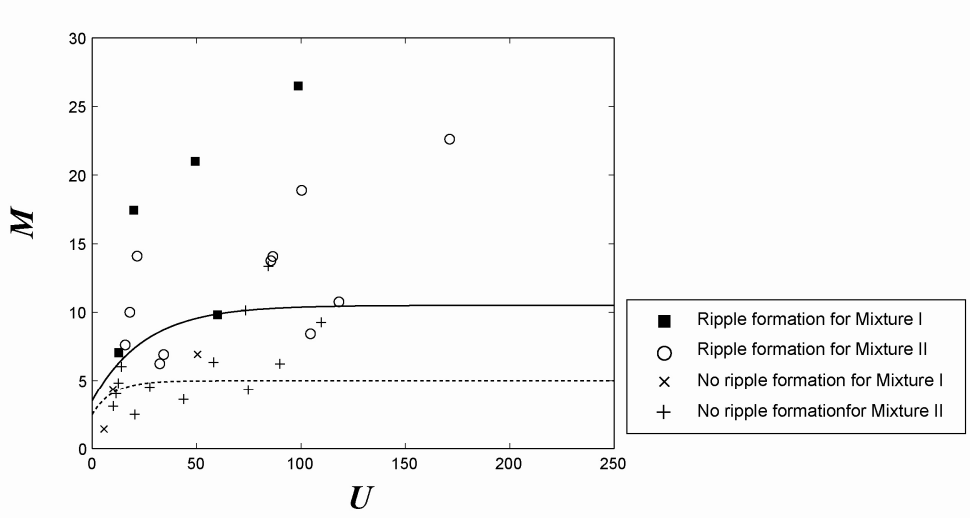

Fig. 6 Mobility numbers, *M*, against Ursell numbers, *U*, in the notched-bed experiments

on them suggested reflecting the magnitude of vortices over ripple surfaces.

As the vortex ripples were developing, they got more symmetrical in some runs. Ripple symmetry index, *i.e.* the ratio of the horizontal length of the stoss side to that of the lee side (Tanner, 1967), increased from 0.40 after 30-min wave action to 0.62 after 60-min in Run MB2_6 and MB2_7 which was the successive experiment of MB2_6 (Fig. 8). The magnitude of vortices over onshore and offshore ripple-surfaces got more symmetrical, and the difference of grain size between onshore-slope and offshore-slope got smaller. These results suggested that the difference of grain size between onshore-slope and offshore-slope depended not only on hydraulic conditions but also on the development of ripple patterns.

Ripples formed on the sand bed had two-dimensional plan forms in most case other than Run MB1_1. In this run, ripple crest alternated three-dimensional plan form called 'brick pattern' (Fig. 9) and two-dimensional plan form. Brick-pattern ripple was often observed at wave-flume experiments (e.g. Bagnold, 1946) and modern shallow-water environments (e.g. Komar, 1973). This plan-form pattern was considered to be formed particularly with small wave-period. However, the mechanisms of change from brick-pattern ripple to two-dimensional ripple and vice versa remain incompletely understood, which requires further study.

4. Summary

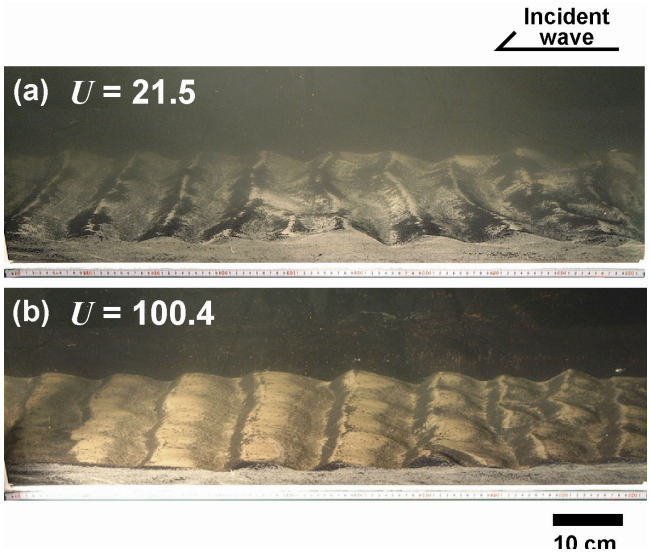

Fig. 7 Photographs of wave ripple formed under (a) U = 21.5 (MB2_18), (b) U = 100.4 (MB2_6). Each photograph was taken after 30-min wave had operated. Waves propagate from right to left

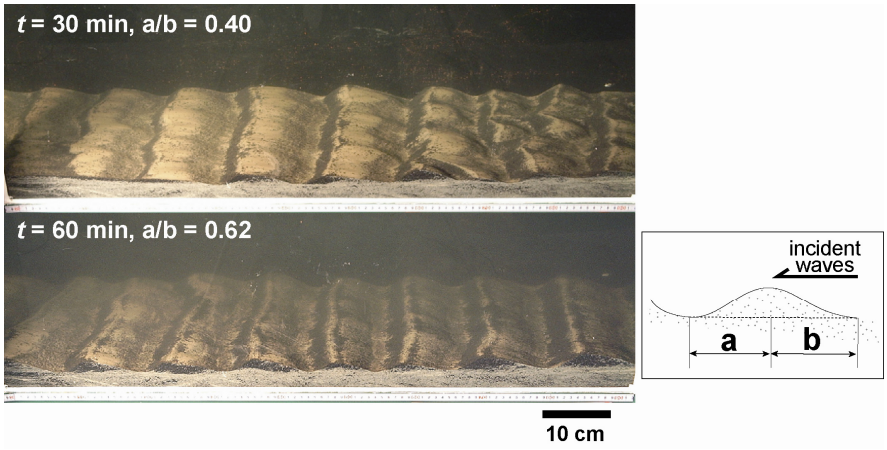

Fig. 8 Photograph of ripples getting more symmetrical geometry along with ripple development

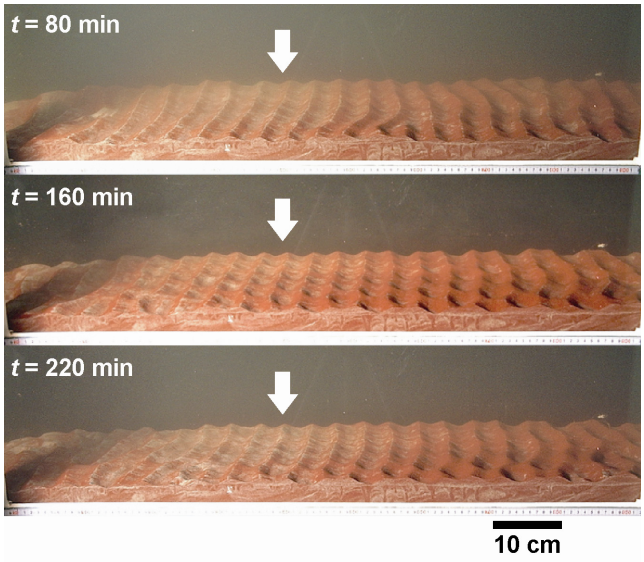

Fig. 9 Photograph of alternation of brick-pattern and 2D ripples (Run MB1_1). Below white arrow, 2D ripples at t = 80 min turned to brick-pattern ripples at t = 160 min, and returned to 2D ripple at t = 220 min

The three series of experiments, a total of 131 runs, were performed with the improved wave flume. The present experiments suggested the follows:

1. Measured H / S_0 in the first series of experiments tended to be smaller than theoretical H / S_0.
2. The critical value of the mobility number for multi-sized sands may be larger than the critical value of the uniform sands.
3. As U-value increasing (i.e. more asymmetrical), the difference of grain size between onshore-slope and offshore-slope appeared more prominently. The coarser sediments deposited on the onshore-side slopes than the offshore-side slopes.
4. As the vortex ripples were developing, they got more symmetrical in some runs, and the difference of grain size between onshore-slope and offshore-slope got smaller.

Revealing mechanism of the suggestion 2–4 require further investigation.

Acknowledgements

The authors appreciate Prof. Fujio Masuda (Doshisha University) for handover of the main body of the wave flume and helpful comments. The authors also thank to Dr. Tomohiro Sekiguchi (University of Tsukuba) for advices about the improvement of the wave flume and useful comments, which enhanced this study.

References

Bagnold, R.A., (1946): Motion of waves in shallow water; interaction between waves and sand bottoms, Proc. Royal Soc. London, 187, series A, pp. 1–15.

Dean, R.G. and Dalrymple, R.A., (1992): Water wave mechanics for engineers and scientists, World Scientific, Singapore, pp. 353.

Dingler, J.R.L., (1975): Wave-formed ripples in nearshore sands, California University, Ph. D. Dissertation, San Diego, pp. 136.

Foti, E., (1993): Grain sorting over ripples: preliminary results of an experimental investigation, In: Belorgey, Rajzona and Sleath (Ed.), Sediment Transport Mechanisms in Coastal Environments and Rivers, World Scientific, Singapore, pp. 311–321.

Foti, E. and Blondeaux, P., (1995): Sea ripple formation: the heterogeneous sediment case, Coastal Engineering, 25, pp. 237–253.

Hughes, S. A., (1993): Physical models and laboratory techniques in coastal engineering, World Scientific, Singapore, pp. 568.

Komar, P.D., (1973): An occurrence of "brick pattern" oscillatory ripple marks at Mono Lake, California, Journal of Sedimentary Petrology, 43, pp. 1111–1113.

Komar, P.D., (1998): Beach processes and sedimentation, Prentice Hall, Upper Saddle River, New Jersey, pp. 544.

Komar, P.D. and Miller, M.C. (1975): The initiation of oscillatory ripple marls and the development of plane-bed at high shear stress under waves, Journal of Sedimentary Petrology, Vol. 45, pp. 697–703.

Lofquist, K.E.B., (1978): Sand ripple growth in an oscillatory-flow water tunnel, U.S. Army Crops of Engineers, Coastal Engineering Research Center, Technical Paper, Washington, DC, No. 78-5, pp. 101.

Naruse, H., (2005): Usage and advantages of an application program STube for settling tube grain-size analysis, Journal of the Sedimentological Society of Japan, 62, pp. 55–61. (In Japanese with English abstract)

Nielsen, P. (1979): Some basic Concepts of wave sediment transport, Series Pap., Technical University of Denmark, Lyngby, 20, pp. 160.

Nielsen, P., (1981): Dynamics and geometry of wave-generated ripples, Journal of Geophysical Research, 86(C7), pp. 707–727.

Sekiguchi, T. and Sunamura, T. (2004): Effects of bed perturbation and velocity asymmetry on ripple initiation: wave-flume experiments, Coastal Engineering, Vol. 50, pp. 231–239.

Sekiguchi, T. and Sunamura, T., (2005): Threshold for ripple formation on artificially roughened beds: wave-flume experiments, Journal of Coastal Research, Vol. 21, pp. 323–330.

Southard, J.B., Lambie, J.M., Federico, D.C., Pile, H.T., and Weidman, C.R., (1990): Experiments on bed configurations in fine sands under bidirectional purely oscillatory flow, and the origin of hummocky cross-stratification, Journal of Sedimentary Petrology, 60, 1–17.

Tanner, W.F., (1967): Ripple mark indices and their uses, Sedimentology, 9, pp. 89–104.

Ursell, F., (1953): The long-wave paradox in the theory of gravity waves, Proceedings of the Cambridge Philogical Society, 49, pp. 685–694.

Wiegel, R.L., (1964): Oceanographical engineering, Prentice Hill, New Jersey, pp. 901.

Appendix

The data set of the first series of experiments are shown in Table A-1, and the one of the second and third in Table A-2.

Table A-1 The data set of the first series.

Run ID	h (cm)	T (s)	S_0 (cm)	H_{max} (cm)	H_{min} (cm)	H_{theory}*1 (cm)	L (m)	kh	U_b (cm/s)	d_o (cm)	R	Remark
FB1_1	40	1.43	16.8	11.1	9.6	16.9	2.4	1.03	20.0	4.5	0.072	—
FB1_2	40	1.43	22.4	14.3	12.6	22.6	2.4	1.03	25.8	5.9	0.063	—
FB1_3	30	1.43	16.8	8.5	7.5	14.1	2.2	0.85	19.6	4.5	0.063	—
FB1_24	55	1.67	21.2	17.5	—	21.6	3.3	1.04	26.8	7.1	—	—
FB1_25	55	2.50	36.4	14.0	—	22.5	5.6	0.62	26.7	10.6	—	—
FB1_26	55	2.86	43.0	16.0	—	22.8	6.5	0.53	31.6	14.4	—	—
FB1_27	55	3.33	48.4	18.5	—	21.7	7.7	0.45	37.6	20.0	—	—
FB1_28	55	4.00	59.0	18.0	—	21.8	9.4	0.37	37.4	23.8	—	—
FB1_29	55	5.00	73.2	22.0	—	21.5	11.8	0.29	46.4	37.0	—	—
FB1_30	45	2.00	41.7	18.0	—	29.7	3.9	0.72	36.3	11.5	—	—
FB1_31	45	1.67	21.2	16.0	—	19.0	3.1	0.90	29.2	7.8	—	—
FB1_32	45	2.22	32.4	16.0	—	20.4	4.5	0.63	33.5	11.9	—	—
FB1_33	45	2.50	36.4	14.0	—	20.0	5.1	0.55	30.3	12.1	—	—
FB1_34	45	2.86	43.0	13.5	—	20.4	5.9	0.48	30.1	13.7	—	—
FB1_35	45	3.33	48.4	19.0	—	19.5	7.0	0.40	43.3	23.0	—	—
FB1_36	45	4.00	36.4	18.0	—	12.1	8.5	0.33	41.7	26.6	—	—
FB1_37	45	5.00	73.2	21.0	—	19.4	10.7	0.26	49.2	39.2	—	—
FB1_38	45	1.43	20.2	14.0	—	21.9	2.5	1.12	22.5	5.1	—	—
FB1_39	45	1.25	15.1	13.0	—	19.5	2.1	1.36	17.9	3.6	—	error*2
FB1_40	45	1.25	14.3	13.0	—	18.4	2.1	1.36	17.9	3.6	—	error
FB1_41	45	1.25	13.4	13.0	—	17.3	2.1	1.36	17.9	3.6	—	error
FB1_42	45	1.25	12.6	11.8	—	16.3	2.1	1.36	16.3	3.2	—	—
FB1_43	45	1.11	10.8	13.0	—	16.1	1.7	1.64	14.8	2.6	—	—
FB1_44	45	1.00	10.5	12.5	—	17.4	1.4	1.96	11.3	1.8	—	error
FB1_45	45	1.00	9.8	11.3	—	16.3	1.4	1.96	10.2	1.6	—	—
FB1_47	35	2.00	41.7	13.5	—	25.6	3.6	0.62	32.3	10.3	—	—
FB1_48	35	1.67	21.2	10.7	—	16.2	2.9	0.77	23.8	6.3	—	—
FB1_50	35	1.43	17.9	10.5	—	16.6	2.3	0.94	21.3	4.8	—	—
FB1_51	35	1.25	12.6	10.5	—	13.8	1.9	1.13	19.0	3.8	—	—
FB1_52	35	1.11	10.8	10.0	—	13.8	1.6	1.35	15.8	2.8	—	—
FB1_53	35	1.00	9.8	10.5	—	14.2	1.4	1.59	14.1	2.2	—	—
FB1_54	35	2.22	32.4	11.3	—	17.7	4.0	0.55	27.8	9.8	—	—
FB1_56	55	10.00	67.5	10.6	5.6	9.9	23.6	0.15	22.6	36.0	0.309	—
FB1_58	55	6.67	72.0	17.6	—	15.8	15.7	0.22	37.5	39.8	—	—
FB1_61	55	5.00	80.5	23.4	19.1	23.6	11.8	0.29	49.4	39.3	0.101	—
FB1_63	55	4.00	70.8	28.4	23.2	26.1	9.4	0.37	59.0	37.6	0.101	—
FB1_64	55	3.33	72.6	25.2	21.0	32.5	7.7	0.45	51.3	27.2	0.091	—
FB1_65	55	2.86	64.5	21.6	—	34.2	6.5	0.53	42.7	19.4	—	—
FB1_66	55	2.50	54.6	18.0	—	33.7	5.6	0.62	34.3	13.7	—	—
FB1_67	55	2.22	48.6	18.5	—	34.4	4.9	0.71	33.8	11.9	—	—
FB1_68	55	1.82	42.0	20.6	17.9	38.1	3.8	0.92	33.7	9.8	0.070	error
FB1_69	55	1.82	36.4	19.1	17.9	33.0	3.8	0.92	31.3	9.0	0.032	error
FB1_70	55	1.82	33.6	19.1	17.2	30.5	3.8	0.92	31.3	9.0	0.052	error
FB1_71	55	1.82	30.8	20.2	17.4	28.0	3.8	0.92	33.1	9.6	0.074	error
FB1_72	55	1.82	28.0	17.9	15.6	25.4	3.8	0.92	29.3	8.5	0.069	error
FB1_73	55	1.82	25.2	17.0	15.6	22.9	3.8	0.92	27.8	8.1	0.043	—
FB1_75	55	1.33	18.0	16.9	16.1	24.3	2.4	1.44	20.0	4.2	0.024	error
FB1_76	55	1.33	17.0	16.4	15.4	22.9	2.4	1.44	19.4	4.1	0.031	—
FB1_77	55	1.25	13.4	17.1	15.6	19.6	2.2	1.60	18.2	3.6	0.046	error
FB1_78	55	1.25	12.6	15.5	14.2	18.4	2.2	1.60	16.5	3.3	0.044	—
FB1_79	55	1.11	11.5	16.8	15.3	19.0	1.8	1.94	13.9	2.5	0.047	error
FB1_80	55	1.11	10.8	15.6	14.6	17.9	1.8	1.94	13.0	2.3	0.033	error
FB1_81	55	1.11	10.1	14.7	13.6	16.7	1.8	1.94	12.2	2.2	0.039	—
FB1_83	55	1.00	9.8	14.1	13.4	17.7	1.5	2.33	8.7	1.4	0.025	—

*1 H_{theory} denotes theoretical wave-height calculated with eq. (5) replaced by measured S_0 and kh.

*2 'Error' remarked at some runs denotes that wave generator could operate for several minutes but stopped within 30-min.

Table A-2 The data set of the second series.

Run ID	h (cm)	T (s)	Hmax (cm)	Hmin (cm)	R	L (m)	kh	Ub (cm/s)	do (cm)	Initial bed	Bedform	λ (cm)	M	U
MB1_1	30	1.25	8.1	8	0.006	1.9	1.01	16.9	6.7	flat bed	Brick-pattern ri	4.4	6.62	10.3
MB1_3	50	2.00	6.8	6.8	0.000	4.1	0.76	12.7	8.1	flat bed	no bedform	—	3.73	9.2
MB1_4	50	2.00	8.8	8.5	0.017	4.1	0.76	16.1	10.3	flat bed	no bedform	—	6.03	11.7
MB1_5	50	2.00	11	10.7	0.014	4.1	0.76	20.2	12.9	flat bed	2D ripple	—	9.49	14.6
MB1_6	50	2.00	10.2	10	0.010	4.1	0.76	18.8	12.0	flat bed	no bedform	—	8.23	13.6
MB1_7	50	2.00	11.2	11	0.009	4.1	0.76	20.7	13.2	flat bed	no bedform	—	9.94	15.0
MB1_8	50	2.00	13.2	12.1	0.043	4.1	0.76	23.6	15.0	flat bed	no bedform	—	12.91	17.1
MB1_9	50	2.00	9.7	9	0.037	4.1	0.76	17.4	11.1	notched bed	2D ripple	7.2	7.05	12.6
MB1_10	50	2.00	4.3	4.1	0.024	4.1	0.76	7.8	5.0	notched bed	no bedform	—	1.42	5.7
MB1_11	50	2.00	7.6	7.1	0.034	4.1	0.76	13.7	8.7	notched bed	no bedform	—	4.36	9.9
MB1_12	50	4.00	9.8	8.8	0.054	8.9	0.35	20.4	25.9	flat bed	no bedform	—	9.60	59.5
MB1_13	50	4.00	12.6	10.7	0.082	8.9	0.35	25.5	32.5	flat bed	no bedform	—	15.07	74.5
MB1_14	50	4.00	8.3	7.5	0.051	8.9	0.35	17.3	22.0	notched bed	no bedform	—	6.93	50.5
MB1_15	50	4.00	9.8	9	0.043	8.9	0.35	20.6	26.2	notched bed	2D ripple	10.1	9.81	60.1
MB1_16	50	4.00	20.3	19.1	0.030	8.9	0.35	43.1	54.9	2D ripple	2D ripple	—	43.09	125.9
MB1_17	50	4.00	20.6	19.3	0.033	8.9	0.35	43.7	55.6	flat bed	no bedform	—	44.19	127.5
MB1_18	50	3.00	8.6	7.5	0.068	6.6	0.48	17.0	16.2	flat bed	no bedform	—	6.70	27.9
MB1_19	50	3.00	12.1	11.2	0.039	6.6	0.48	24.6	23.5	flat bed	2D/3D ripple	10.5	14.04	40.4
MB1_20	50	1.25	16.2	14.4	0.059	2.1	1.48	18.5	7.4	flat bed	2D ripple	4.6	7.92	5.5
MB1_21	50	3.00	15	13.5	0.053	6.6	0.48	30.1	28.8	notched bed	2D ripple	—	21.00	49.4
MB1_22	50	2.00	15.6	13.8	0.061	4.1	0.76	27.4	17.5	notched bed	2D ripple	8.6	17.43	19.8
MB1_23	50	4.00	16.1	14.8	0.042	8.9	0.35	33.8	43.1	notched bed	2D ripple	—	26.51	98.8
MB2_1	50	4.00	7.4	6.3	0.080	8.9	0.35	15.0	19.1	notched bed	no bedform	—	3.59	43.8
MB2_2	50	4.00	9.6	8.6	0.055	8.9	0.35	19.9	25.4	notched bed	no bedform	—	6.34	58.2
MB2_3	50	4.00	11.9	11.1	0.035	8.9	0.35	25.2	32.1	notched bed	no bedform	—	10.13	73.5
MB2_4	50	4.00	14.1	12.7	0.052	8.9	0.35	29.3	37.4	notched bed	2D ripple	11.9	13.76	85.7
MB2_5	50	4.00	14.7	12.4	0.085	8.9	0.35	29.7	37.8	notched bed	2D ripple	10	14.07	86.6
MB2_6	50	4.00	17.4	14	0.108	8.9	0.35	34.4	43.8	notched bed	2D ripple	13.4	18.88	100.4
MB2_7	50	4.00	17.4	14	0.108	8.9	0.35	34.4	43.8	2D ripple	2D ripple	12.9	18.88	100.4
MB2_8	50	3.00	6.6	5.2	0.119	6.6	0.48	12.5	11.9	notched bed	no bedform	—	2.48	20.5
MB2_9	50	3.00	8.7	7.2	0.094	6.6	0.48	16.8	16.0	notched bed	no bedform	—	4.51	27.6
MB2_10	50	3.00	10.1	8.6	0.080	6.6	0.48	19.8	18.9	notched bed	2D ripple	—	6.24	32.4
MB2_11	50	3.00	10.6	9.1	0.076	6.6	0.48	20.8	19.9	notched bed	2D ripple	11.7	6.92	34.2
MB2_12	50	2.00	7.9	7	0.060	4.1	0.76	13.9	8.9	notched bed	no bedform	—	3.09	10.1
MB2_13	50	2.00	9.1	7.9	0.071	4.1	0.76	15.9	10.1	notched bed	no bedform	—	4.02	11.5
MB2_14	50	2.00	10	8.6	0.075	4.1	0.76	17.4	11.0	notched bed	no bedform	—	4.81	12.5
MB2_15	50	2.00	11.1	9.7	0.067	4.1	0.76	19.4	12.4	notched bed	no bedform	—	6.02	14.0
MB2_16	50	2.00	12.3	11.1	0.051	4.1	0.76	21.8	13.9	notched bed	2D ripple	—	7.62	15.8
MB2_17	50	2.00	14.2	12.6	0.060	4.1	0.76	25.0	15.9	notched bed	2D ripple	10.8	9.99	18.1
MB2_18	50	2.00	16.7	15.1	0.050	4.1	0.76	29.7	18.9	notched bed	2D ripple	12.5	14.07	21.5
MB2_19	50	5.00	8.3	6.5	0.122	11.2	0.28	16.4	26.1	notched bed	no bedform	14.9	4.31	74.8
MB2_20	50	5.00	11.1	9.6	0.072	11.2	0.28	23.0	36.6	notched bed	2D ripple	13	8.43	104.6
MB2_21	50	5.00	9.7	8.1	0.090	11.2	0.28	19.7	31.4	notched bed	no bedform	—	6.23	90.0
MB2_22	50	4.00	13.8	12.6	0.045	8.9	0.35	28.9	36.8	notched bed	no bedform	—	13.35	84.4
MB2_23	50	5.00	11.6	10.1	0.069	11.2	0.28	24.1	38.3	notched bed	no bedform	—	9.26	109.7
MB2_24	50	5.00	12.4	11	0.060	11.2	0.28	26.0	41.3	notched bed	2D ripple	—	10.77	118.3
MB2_25	50	5.00	17.8	16.1	0.050	11.2	0.28	37.6	59.9	notched bed	2D ripple	13.4	22.61	171.3

混合粒径砂を用いたリップルの形成と分級過程：造波水槽による予備実験

山口直文*・関口秀雄

*京都大学大学院理学研究科

要　旨

造波水槽の性能と，混合粒径砂がリップル形成に与える影響を調べるために，3 組の実験を行った。最初の一連の実験では，固定床を用いて造波水槽の性能評価を行った。その結果，波高/造波板ストロークの比が予想値よりやや小さい値を持つことがわかった。その他の 2 組の実験では，混合粒径砂の砂床を設置して実験を行い，次の二つのことが明らかになった。(1) 混合粒径砂では，均一粒径砂の時よりもリップル発生し始める mobility number が大きい。(2)流速の岸沖方向での非対称性に応じて，リップルの岸側斜面と沖側斜面の粒径が異なる。

キーワード：ウェーブリップル，造波水槽実験，混合粒径砂，非対称振動流，粒度分級